Journal of
Ship&Ocean
Technology
©DECEMBER 2003

SOTECH Vol. 7, No. 4, pp. 32~40, 2003

Numerical Study of Ejected Droplet Formation in Two-Liquid System

Mu-Seok Song[1], Shunji Homma[2] and Haruhisa Honda[2]

[1]Hongik University, Jochiwon, Korea; E-mail: msong@hongik.ac.kr
[2]Saitama University, Saitama, Japan

Abstract

Numerical simulation code is developed to study the formation of liquid drops from a nozzle into another quiescent liquid. The Navier-Stokes equations for two immiscible, incompressible, Newtonian fluids are solved on a fixed, staggered grid of cylindrical axisymmetric coordinates. Interfacial motion is captured using a Front-Tracking Method. The time variation of interfacial shape simulated by the code is in excellent agreement with experiments. Simulation results show that the viscosity ratio affects the size of the satellite drops.

Keywords: droplet formation, front-tracking, two-liquid system, satellite drop

1 Introduction

Estimation of the size of drops is an essential first step for the design of industrial drop dispersion equipments. The formation of drops from jets (Bogy 1979) and sheets (Taylor 1959) has been studied extensively for many years. Recent commercial success includes the application of drop formation in ink jet printing, and this technology has the capabilities to be used as a feeding device for micro fluidic systems and as a spotting method for DNA micro array (Okamoto et al 2000). In this drop-on-demand situations, dripping mode, where drop detaches near a nozzle, is of more interest than the jetting mode, where a jet issued from a nozzle breaks up into drops far away from the nozzle.

Dripping mode can be classified into two regimes: periodic dripping and quasi-periodic dripping (Clanet and Lasheras 1999). For periodic dripping, the size of the drops can be estimated from surface tension, viscosity, and diameter of the orifice assuming quasi-steady state without inertial effect. This is widely used for determining surface tension where it is known as the drop weight method (Harkins and Brown 1919). Quasi-periodic dripping is often called Dripping Faucet regime and has been extensively studied as an example of a non-linear dynamics showing chaotic attractor (Martien et al 1985).

Direct numerical simulation (DNS) for dripping mode already appeared in the mid-1980's for the design of ink jet printing devices (Fromm 1984). Since then, the simulations of the dripping mode have improved remarkably. Some of examples are as follows: Asai(1992) conducted three dimensional calculations with a VOF method and successfully simulated whole cycle of bubble jets, namely, the bubble growth inside the chamber of the nozzle, the ejection of the ink, the rapid shrinking of the bubble, and the formation of an ink drop. Wilkes et al(1999) has developed a

sophisticated finite element code to simulate the dynamic motion for both primary drops and a microthread that eventually disintegrated into small satellite drops. This code was utilized for the study of a chaotic dripping phenomenon (Ambravaneswaran et al 2000).

Since ambient air does not influence drop motion under normal circumstances such as in ink jet printing and when water drips from a faucet, most studies of the dripping mode ignore the effect of the external flow. For liquid-liquid systems, however, the ambient fluid does affect the break off of the drops and their motion. Thus the effect of external flow can no longer be neglected even when the ambient flow is initially stationary. Scheele and Meister(1968) established a theory to predict the volume of the primary drops at low velocities by extending the theory of Harkins and Brown(1919) for dripping liquid in air. Richards et al(1995) developed a DNS code with VOF method for jetting and dripping modes in liquid-liquid systems, and demonstrated that the computed sizes of drops are in reasonably good agreement with what is observed in experiments (Scheele and Meister 1968, Meister and Scheele 1969). Xiaoguang(1999) applied Richards' code to the dripping mode in liquid-liquid systems and carried out systematic numerical experiments especially paying attention to the effect of external flow on the breakup length of the jet. Although codes have been developed for jetting and dripping modes, there are still many unresolved issues in liquid-liquid systems such as non-linear dynamics including chaotic modes of breakup, and scalings of pinch-off (Lister and Stone 1998). It is also important for practical applications to be able to simulate drop-on-demand situation, where a pulse-like injection is applied to the flow at the nozzle.

Our goal is to develop a reliable numerical code for the dripping mode. So far we have developed a simulation code with a Front-Tracking / Finite Difference Method (FT-FDM) (Unverdi and Tryggvason 1992), and successfully simulated drop formation for the jetting mode (Homma et al 2002). However, no dripping mode has been simulated so far with the FT-FDM due to somewhat unphysical boundary condition used at the nozzle exit where parabolic velocity distribution has always been specified. For the jetting mode, this boundary condition works properly, since the influence of the break-off on the flow is limited far from the exit of the nozzle. For the dripping mode, on the other hand, the flow in the vicinity of the nozzle lip is influenced by the break-off of the drops; the flow sometime penetrates into the nozzle when breakup happens close to the nozzle lip. To remedy the boundary condition in this case, a running section of the nozzle should be included as in the Richards' code (Richards et al 1995), and parabolic velocity distribution should be given at the bottom of the running section. If certain length of the running section is taken, the fixed velocity distribution at the boundary does not disturb the flow at the exit of the running section.

In this article, we describe how our code is modified and demonstrate the validity of the code by comparing the computational results with our own experiments (Song et al 1999, Song 2003). Then, we present some simulation results for the dripping mode with several viscosity ratios.

2 Mathematical formulation and numerical method

A fluid of ρ_d and μ_d is injected into another immiscible quiescent fluid of ρ_c and μ_c through a nozzle with L_N and R_N , and eventually disintegrated into drops as shown in Figure 1. Here, ρ and μ are density and dynamic viscosity, respectively, and subscripts c and d represent the continuous phase and the dispersed phase (drop), respectively. L_N and R_N are nozzle length and

radius, respectively. g is the gravitational acceleration.

Both fluids are assumed to be immiscible, incompressible, and Newtonian. It is also assumed that the system is isothermal and the interface is completely clean, so that the interfacial tension is constant. The governing equations under these assumptions are the momentum equation

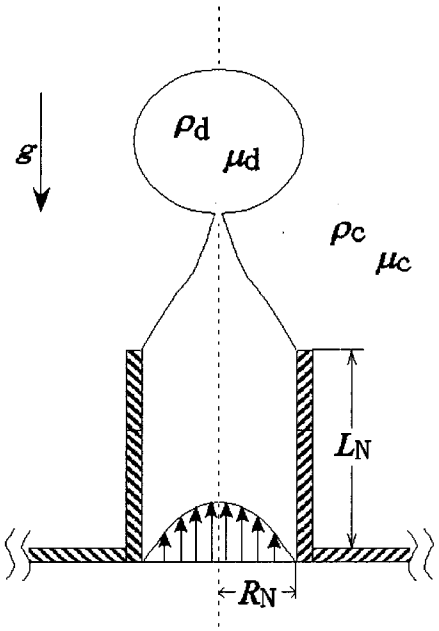

Figure 1: Sketch of the formation of a drop from a nozzle

$$\frac{\partial}{\partial t}\rho u + \nabla \cdot \rho u u = \nabla P + \nabla \cdot \mu(\nabla u + \nabla u^T) + \rho f + \int_f \sigma \kappa n_f \delta(x - x_f) dA_f \tag{1}$$

the continuity equation

$$\nabla \cdot u = 0 \tag{2}$$

and the equations of state for the density and viscosity

$$\frac{D}{Dt}\rho = \frac{D}{Dt}\mu = 0 \tag{3}$$

In the above equations, u is velocity vector; P is pressure; f is body force; σ is interfacial tension; κ is twice the mean curvature of the interface; n_f is unit normal at the interface; x is position vector; x_f is position at interface; A_f is interfacial area.

The interfacial tension is taken into account by the delta function, which is zero everywhere except at the interface. Since the flow is almost entirely axisymmetric for the dripping mode in quiescent fluid, cylindrical axisymmetric coordinates are good enough to discretize the governing equations with finite difference approximations. The computational domain is right half of Figure 1. The right side of the domain and the bottom outside the nozzle are full-slip boundaries. The left and the top of the domain are symmetry and outflow boundary conditions, respectively. Fully

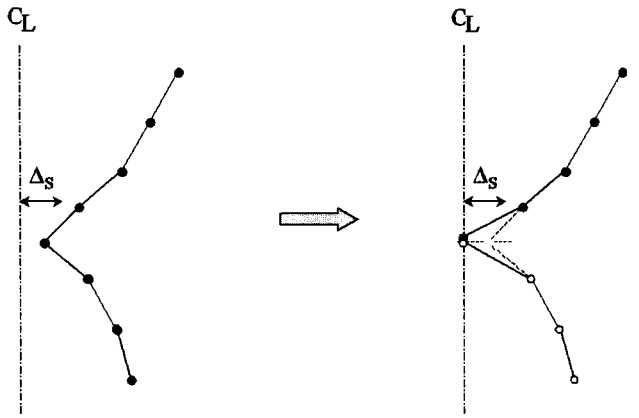

Figure 2: Illustration of the algorithm for front rupture

developed parabolic velocity distribution with an average velocity of u_0 is given at the bottom of the running section. For the surface of the running section, no-slip boundary conditions are given implicitly rather than specifying the velocity zero. We arrange the running section as an obstacle in the computational domain, and adjust the pressure in the obstacle as the velocities on the surface become zero. By this technique, which has already been applied to the problem of molten metal solidification (Che 1999), the geometry of the nozzle can be changed without rebuilding the grid structure. Furthermore, accumulated knowledge of the FT-FDM such as multigrid solver, can be directly used. The details of this technique can be found in (Honda 2003).

The interfaces are traced by sets of many small elements, that is, fronts. The fronts are superimposed on a fixed Eulerian grid for the flow variables. This Front-Tracking method has been applied to various flow problems with free interfaces. For a detailed description of the Front-Tracking method and its applications, see Tryggvason(2001). Here, specific treatments for the formation of drops from a nozzle are summarized.

At $t = 0$, a flat interface covers the exit of the running section of the nozzle, so a straight line of the front is put from the lip of the nozzle to the axis of symmetry. The right edge of the front at the lip is pinned, but the left edge on the axis of symmetry moves with the local velocity. When a drop breaks off, the front must be separated into two independent fronts. The algorithm of the front separation is illustrated in Figure 2. The front is divided if a node of an element comes within a very small distance Δs, threshold of pinch-off, from the axis of symmetry. The node is moved to the axis of symmetry, then the front is cut into two fronts. The size of Δs was chosen as half of the grid interval, and, as shown later, is small enough to simulate both primary and satellite drops.

3 Experiment

The experimental result (Song et al 1999, Song 2003) was obtained in a water-kerosene system. A nozzle ($R_N = 4.7mm$ and $L_N = 152.5mm$) was set vertically in the bottom of a container filled with water. A dispersed phase of kerosene was injected upward with $u_0 = 6.0 \times 10^{-3} m/s$. A high-speed camera with 400 frames per second is used to record the dynamic motion of liquid-liquid interfaces. The physical properties are summarized in Table 1.

Table 1: Physical properties of water-kerosene system

	Dispersed Phase Kerosene(Drop)	Continuous Phase Water
ρ $[kg/m^3]$	809	992
μ $[Pa \cdot s]$	2.30×10^{-3}	1.04×10^{-3}
σ $[N/m]$	0.0365	

Table 2: Comparison of drop sizes

	Primary drop $[mm^3]$	Satellite drop $[mm^3]$
Experimental	482	1.70
Computational	477	1.75
Error [%]	1.04	2.94

4 Results and discussions

4.1 Code validation

Figure 3 shows dynamics of the formation of a drop from a nozzle. The interface rises with dome-like shape (a), then a neck forms (b). A drop breaks off at the neck, and just after the break-off the rest of the body has a conical shape (c). The tip of the cone, where the interfacial tension is very high, moves back to the nozzle due to the high capillary pressure, then bounces back again. This rebound results in the form of a small satellite drop (d). Both primary and satellite drops rise due to inertial and buoyancy forces [(e) and (f)].

Simulation result (left hand side of each frame) is obtained with 128×768 uniform grid meshes. Corresponding non-dimensional numbers are: $Re = 19.8$, $We = 0.007$, $Fr = 3.6 \times 10^{-4}$, and $\lambda = 0.453$. Here, Reynolds number (Re) is defined by $2R_N u_0 \rho_d / \mu_d$, Weber number (We) is defined by $2R_N u_0^2 \rho_d / \sigma$ and Froude number (Fr) is defined by $u_0^2 / 2R_N g$. λ is the viscosity ratio (μ_c / μ_d).

Although the location of the satellite drop is slightly different [(d) and (e)], the simulated interfacial shape is in almost exact agreement with experimental one (right hand side). Furthermore, the sizes of both primary and satellite drops are identical between simulation and experiment as shown in Table 2. The slight difference of the location of the satellite can be fixed if either an adaptive grid generation (Agresar et al 1998) or a precise algorithm of a front rupturing based on a pinch-off scaling (Lister and Stone 1998) is included. We are currently working on the latter approach, in particular, finding scaling relations in two viscous fluid systems for finite Reynolds number (Homma et al 2000). Even though the simple rupture algorithm mentioned earlier is used, however, the result is convincing and the code developed in this study is applicable to numerical experiments for the dripping mode.

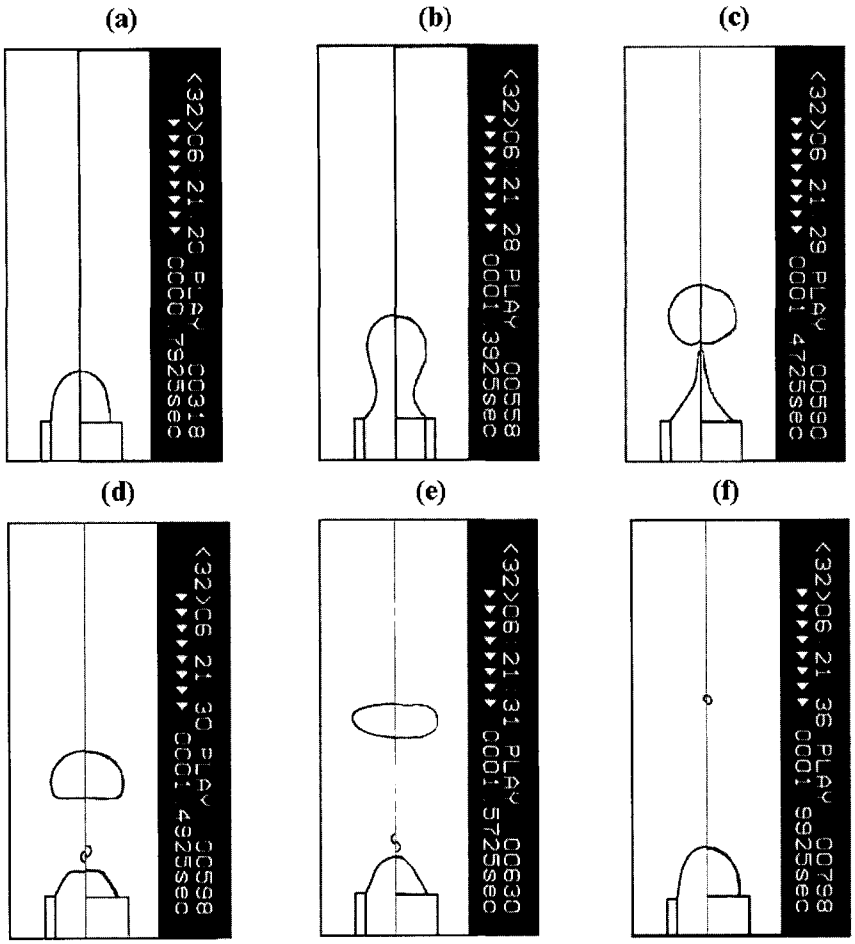

Figure 3: A sequence of drop formation from a nozzle, left : simulation, right : experimental

4.2 Effect of the viscosity ratio

Using the code developed here, we examine the effect of the viscosity ratio on the drop formation. The Reynolds, Weber, and Froude numbers are fixed at the same values as in Figure 3. Figure 4 shows the time change of the position of the interface at the axis of symmetry. The embedded pictures are the corresponding shapes of the periods (A) $\sim$ (D). The bottom frame is a magnified view for the period (D). For period (A), the interface develops almost linearly with dome-like shape. After the neck forms (B), the rise of the bulb accelerates, then the neck pinches off at the first blank of the lines. The cusp behind the primary drop moves back to the nozzle (C), then a satellite forms at the second blank of the lines. The rest of the body develops with oscillation (D). The oscillation eventually damps, then the same cycle begins. For $\lambda = 0.5$ and 1.0, the profiles are almost identical. For $\lambda = 20$, where the continuous phase is 20 times more viscous than the dispersed one, the rise of the bulb is a little slower [see, period (B)] and the relaxation time of the oscillation is shorter [see, period (D)] than for the other two cases. The viscous continuous phase retards the rise of the bulb and damps the oscillation. Table 3 shows the sizes of the primary

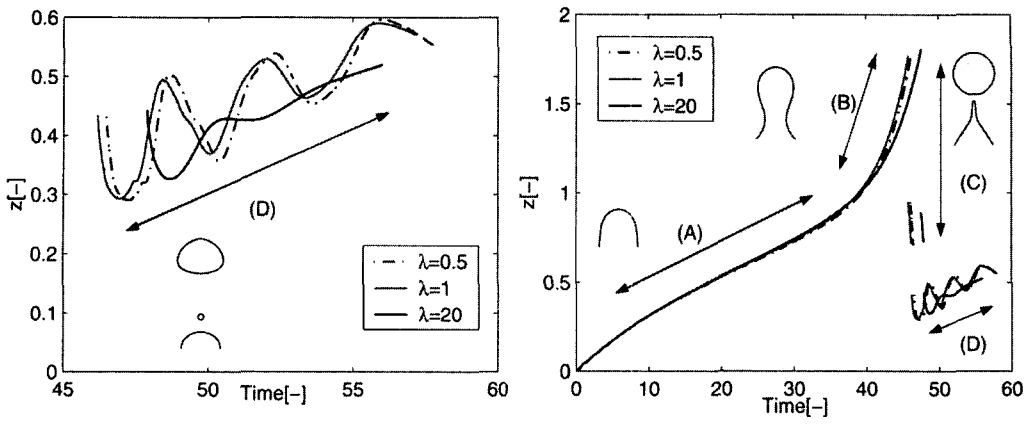

Figure 4: The position of the interface at the axis of symmetry (Re=19.8, We=0.007, and Fr=3.9×10^{-4})

Table 3: The effect of viscosity ratio on the drop sizes

λ	Primary drop [mm^3]	Satellite drop [mm^3]
0.50	478	1.76
1.00	481	1.73
20.0	527	1.07

and the satellite drops. For both primary and satellite drops, there are no significant differences between $\lambda = 0.5$ and 1.0. For $\lambda = 20$, however, the primary drop is bigger and the satellite drop is smaller than those for $\lambda = 0.5$ and 1.0. The slow rise of the bulb results in the bigger primary drop. The size of the satellite drop may be related to the intensity of the oscillation; If the shock due to the backflow of the cusp is absorbed and no oscillation occur, a satellite does not form. Since the viscous continuous phase works as the damper for the oscillation, the size of the satellite drop decreases with increasing the external viscosity.

5 Concluding remarks

Drop formation from a nozzle in another immiscible liquid is successfully simulated for the dripping mode. By including a running section of the nozzle, excellent agreement of interfacial motion is achieved between simulations and experiments. Numerical experiments where the viscosity ratio is changed show that, when the continuous phase is more viscous than the dispersed phase, the formation of the satellite drop is affected by the viscosity ratio.

Acknowledgment

This work was partially supported by Advanced Ship Engineering Research Center of the Korea Science & Engineering under R11-2002-104-02005-0.

References

AGRESAR, G., LINDERMAN, J. J., TRYGGVASON, G. AND POWELL, K. G. 1998 An adaptive, cartesian, front-tracking method for the motion, deformation and adhesion of circulating cells. J. of Computational Physics, **143**, pp. 346-380

AMBRAVANESWARAN, B., PHILLIPS, S. D. AND BASARAN, O. A. 2000 Theoretical analysis of a dripping faucet. Physical Review Letters, **85**, pp. 5332-5335

ASAI, A. 1992 Three-dimensional calculation of bubble growth and drop ejection in a bubble jet printer. J. of Fluids Engineering, **114**, pp. 638-641

BOGY, D. B. 1979 Drop formation in a circular jet. Annual Review of Fluid Mechanics, **11**, pp. 207-228

CHE, J. 1999 Numerical simulations of complex multiphase flows: Electrohydrodynamics and solidification of droplets. Ph.D. thesis, University of Michigan, Ann Arbor, MI.

CLANET, C. AND LASHERAS, J. 1999 Transition from dripping to jetting. J. of Fluid Mechanics, **383**, pp. 307-326

FROMM, J. E. 1984 Numerical calculation of the fluid dynamics of drop-on-demand jets. IBM J. of Research and Development, **28**, **3**, pp. 322-333

HARKINS, W. D. AND BROWN, F. E. 1919 The determination of surface tension (free surface energy), and the weight of falling drops: the surface tension of water and benzene by the capillary height method. J. of American Chemical Society, **41**, pp. 499-524

HOMMA, S., KOGA, J., MATSUMOTO, S. AND TRYGGVASON, G. 2000 Pinch-off dynamics of jet breakup in liquid-liquid systems. Proc. 2000 ASME Fluids Engineering Division Summer Meeting. FEDSM00-11278(CDROM)

HOMMA, S., KOGA, J., MATSUMOTO, S. AND TRYGGVASON, G. 2002 Formation of a jet and its breakup into drops in liquid-liquid systems. Theoretical and Applied Mechanics, **51**, pp. 241-250

HONDA, H. 2003 CFD visualization of drop generation from a nozzle. Manuscript for Student Paper Contest of 4th ASME/JSME Joint Fluids Engineering Conference

LISTER, J. R. AND STONE, H. A. 1998 Capillary breakup of a viscous thread surrounding by another viscous fluid. Physics of Fluids, **10**, pp. 2758-2764

MARTIEN, P., POPE, S. C., SCOTT, P. L. AND SHAW, R. S. 1985 The chaotic behavior of the leaky faucet. Physics Letters, **110A**, pp. 399-404

MEISTER, B. J. AND SCHEELE, G. F. 1969 Drop formation from cylindrical jets in immiscible liquid systems. AIChE Journal, **15**, **5**, pp. 700-706

OKAMOTO, T., SUZUKI, T. AND YAMAMOTO, N. 2000 Microarray fabrication with covalent attachment of DNA using bubble jet technology. Nature Biotechnology, **18**, pp. 438-441

RICHARDS, J. R., BERIS, A. N. AND LENHOFF, A. M. 1995 Drop formation in liquid-liquid systems before and after jetting. Physics of Fluids, **7**, **11**, pp. 2617-2630

SCHEELE, G. F. AND MEISTER, B. J. 1968 Drop formation at low velocities in liquid-liquid systems. AIChE Journal, **14**, **1**, pp. 9-19

SONG, M., HOMMA, S. AND HONG, K. 1999 Formation of oil drops discharged underwater. Proc. 9th International Offshore and Polar Engineering Conference, **I**, pp. 390-396

SONG, M. 2003 An experimental investigation of the underwater oil drop formation. J. of Korean Society for Marine Environmental Engineering, **6**, **1**, pp. 3-10

TAYLOR, G. 1959 The dynamics of thin sheets of fluid III. disintegration of fluid sheets. Proc.

of the Royal Society A, **253**, pp. 313-321

TRYGGVASON, G., BUNNER, B., ESMAEELI, A., JURIC, D., AL-RAWAHI, N., TAUBER, W., HAN, J., NAS, S. AND JAN, Y. 2001 A front-tracking method for the computations of multiphase flow. J. of Computational Physics, **169**, pp. 708-759

UNVERDI, S. O. AND TRYGGVASON, G. 1992 A front tracking method for viscous, incompressible, multi-fluid flows. J. of Computational Physics, **100**, pp. 25-37

WILKES, E. D., PHILLIPS, S. D. AND BASARAN, O. A. 1999 Computational and experimental analysis of dynamics of drop formation. Physics of Fluids, **11**, pp. 3577-3598

XIAOGUANG, Z. 1999 Dynamics of drop formation in viscous flows. Chemical Engineering Science, **54**, pp. 1759-1774